Accepted (peer-reviewed) version

Zero-dimensional hybrid organic-inorganic lead halides and their post-synthesis reversible transformation into 3D perovskites

Bas A. H. Huisman, Francisco Palazon,* and Henk J. Bolink

Instituto de Ciencia Molecular, Universidad de Valencia, C/ Catedrático J. Beltrán 2, 46980, Paterna, Spain. E-mail: francisco.palazon@uv.es

ABSTRACT: Zero-dimensional mixed-halide hybrid organic-inorganic $MA_4PbX_6 \cdot 2H_2O$ ($MA=CH_3NH_3^+$; $X=Br_{1-x}I_x$ with $0<x<1$) have been synthesized by a solvent-free mechanochemical approach. It has been shown that this 0D phase with sharp absorption features in the near-UV is a hydrated structure, which can be reversibly transformed into the 3D perovskite phase $MAPbX_3$ by simple thermal annealing (dehydration) in air. This work reveals a new approach to hybrid organic-inorganic perovskites and related zero-dimensional structures which have so far only been thoroughly studied for the inorganic Cs_4PbX_6 compounds.

INTRODUCTION:

Inorganic and hybrid organic-inorganic ternary lead halides can exist in different stoichiometries and crystal structures.[1] $APbX_3$ perovskites with A being either an alkali metal cation (*e.g.*, Cs^+) or a small organic cation (*e.g.,* $MA=(CH_3NH_3)^+$ or $FA=CH(NH_2)_2^+$) and X a halide anion (*e.g.*, Cl^-, Br^-, or I^-) are by far the most studied class of ternary metal halides, owing to their exceptional optoelectronic properties.[2–4] Nevertheless, other phases such as A_4PbX_6 or the dihydrate $A_4PbX_6 \cdot 2H_2O$ have also been reported. These can be viewed as zero-dimensional analogues to the 3D perovskites, based on the degree of connectivity between adjacent $[PbX_6]^{4+}$ octahedra[5] (see Figure 1).

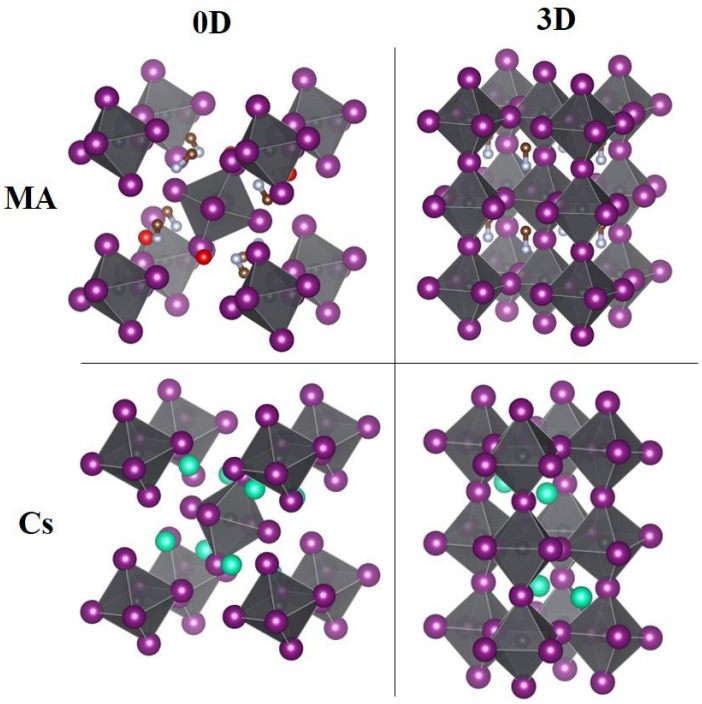

Figure 1. Crystal structures of $MA_4PbI_6{\cdot}2H_2O$ (top left), $MAPbI_3$ (top right), Cs_4PbBr_6 (bottom left), and $CsPbBr_3$ (bottom right) drawn with VESTA software based on reference crystallographic information files retrieved from the Inorganic Crystal Structure Database (refs: 162158, 97851, and 110630) and the Crystallography Open Database (ref: 4335638). The two structures on the left can be considered as zero-dimensional based on the isolated $[PbX_6]^{4+}$ octahedra while the two structures on the right can be considered three-dimensional distorted perovskites. Note that these are the most commonly-reported structures for the aforementioned compounds in ambient conditions, but both $MAPbI_3$ and $CsPbBr_3$ convert to the so-called perfect cubic perovskite structure at high temperature.

While inorganic Cs_4PbX_6 have been extensively studied in the last 3-4 years,[6–11] it is striking to note that only very few reports have focused on the MA- or FA-based hybrid organic-inorganic analogues.[12,13] Yet, the existence of the dihydrate $MA_4PbI_6{\cdot}2H_2O$ is known at least since 1987,[14] and other recent articles have noted the occurrence of this phase, mostly as a degradation or side-product of the 3D perovskite counterpart.[15,16] In fact, one of the main reasons why zero-dimensional ternary metal halides are under study, is not only their intrinsic properties such as sharp absorption features in the near-UV (which could pave the way to their implementation as narrow-band UV photodetectors) but their possible interconversion into perovskites. For inorganic Cs-Pb-X compounds, an extensive literature has developed in the past few years on reversible and irreversible phase transformations under different physical and chemical stimuli.[17–21] Only recently, these transformations have been

rationalized in terms of the Cs^+ cation substructure.[1] The conservation of this (slightly distorted) cationic substructure is thought to be key in the interconversion of PbX_2-rich (here $APbX_3$) and PbX_2-poor (here A_4PbX_6) phases. Hence, it is important to study the possibility of such interconversion with another monovalent cation, especially a small organic molecule. This is particularly important as the majority of lead halide perovskites used in optoelectronics are based on such organic cations. Furthermore, it is important to highlight that the reported hybrid organic-inorganic zero-dimensional phase is in fact a hydrated structure: $MA_4PbX_6 \cdot 2H_2O$ (note the oxygen atoms from H_2O molecules represented by red balls in Figure 1; hydrogen atoms are not shown).[14] This added complexity also provides another possible key to the control of crystalline structures in hybrid organic-inorganic lead halides through the addition or removal of water (moisture).

Hereafter we will show the first solvent-free mechanochemical synthesis of $MA_4PbI_6 \cdot 2H_2O$ and demonstrate its reversible transformation into and from the 3D perovskite analogue ($MAPbI_3$) by controlled (de)hydration under thermal annealing and simple cool-down in moist air. Finally, we will demonstrate the synthesis of mixed $MA_4Pb(Br_{1-x}I_x)_6 \cdot 2H_2O$ with $0<x<1$, thus expanding the possibilities of these overlooked hybrid organic-inorganic ternary metal halides, which could be implemented for instance in tunable narrow-band near-UV photodetectors.

RESULTS AND DISCUSSION:

In order to investigate zero-dimensional hybrid organic-inorganic lead halides, MAI and PbI_2 powders have been ball-milled in 4:1 molar ratio in air (relative humidity around 40%-60%; see experimental section for more details). This simple mechanochemical approach has been demonstrated to be very efficient for the synthesis of different metal halide semiconductors and phosphors.[22] In particular, it has been implemented for the synthesis of the inorganic analogues Cs_4PbX_6.[23] Figure 2a shows the X-ray diffraction data of the as-obtained powders together with the calculated signal from whole-pattern

deconvolution following Le Bail fit procedure. The fit is obtained considering a $P2_1/c$ space group (monoclinic system) with unit cell parameters detailed in Table 1.

Table 1. Calculated and reference unit cell parameters of $MA_4PbI_6 \cdot 2H_2O$.

Space group: $P2_1/c$ (14)	This work	Reference (ICSD:110630) [14]
a (Å)	10.469	10.421
b (Å)	11.363	11.334
c (Å)	10.701	10.668
α (º)	90	90
β (º)	91.76	91.73
γ (º)	90	90

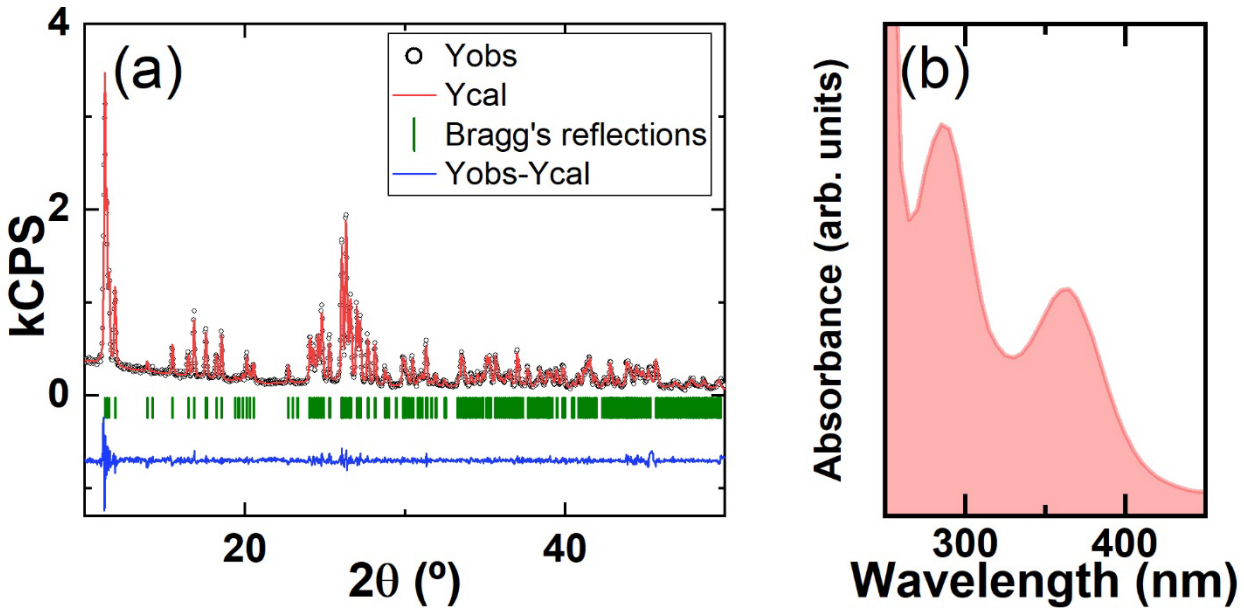

Figure 2. (a) XRD observed and calculated data of MA_4PbI_6 powder. (b) Optical absorption spectrum of a dilute dispersion of $MA_4PbI_6 \cdot 2H_2O$ in a 1:3 ethanol:hexane mixture.

As can be observed, the match between the observed and calculated XRD signal is very close, pointing out to the high purity of the mechanochemically synthesized zero-dimensional phase. Also, the unit cell parameters are in close agreement with the values reported by Vincent et al. from solution synthesis[14] (see Table 1). It is important to notice that when the salt precursors are ball-milled in dry

nitrogen in the same 4:1 ratio, full conversion into the desired $MA_4PbI_6 \cdot 2H_2O$ phase is not achieved (see Figure S1). This highlights the importance of moisture in the formation of the zero-dimensional hybrid organic-inorganic phase, which is an important difference with the inorganic analogue Cs_4PbI_6.

Optical absorption measurements were carried out on the as-synthesized powders dispersed in a 1:3 ethanol:hexane mixture (see experimental section for details). Figure 2b reveals two sharp absorption peaks at 288nm and 364nm, very similar to what is observed in the absorption spectrum of Cs_4PbI_6.[19] Indeed, due to the zero-dimensional structure of these compounds (see Figure 1), the optical absorption is related to the electronic configuration of isolated $[PbI_6]^{4+}$ octahedra. Hence, the role of the monovalent cation, and in this case of the water molecules, is only to preserve the structural stability. An ongoing debate on the much-more studied inorganic counterparts is centered on the possible photoluminescence (PL) from these 0D phases. While some have claimed that these do not show PL (and ascribed observed signals to traces of 3D-phase impurities) others have attributed visible PL (at least in the case of bromide compounds) to self-trapped excitons or other intrinsic features of the 0D phase.[6,24] We, however, could not observe any PL from these materials.

As previously explained, part of the interest on zero-dimensional ternary lead halides arises from their possible conversion into 3D perovskites which are relevant for photovoltaics and other optoelectronic applications. Here, we conducted XRD of the as-synthesized $MA_4PbI_6 \cdot 2H_2O$ powders while thermally annealing *in-situ* (Figure 3a).

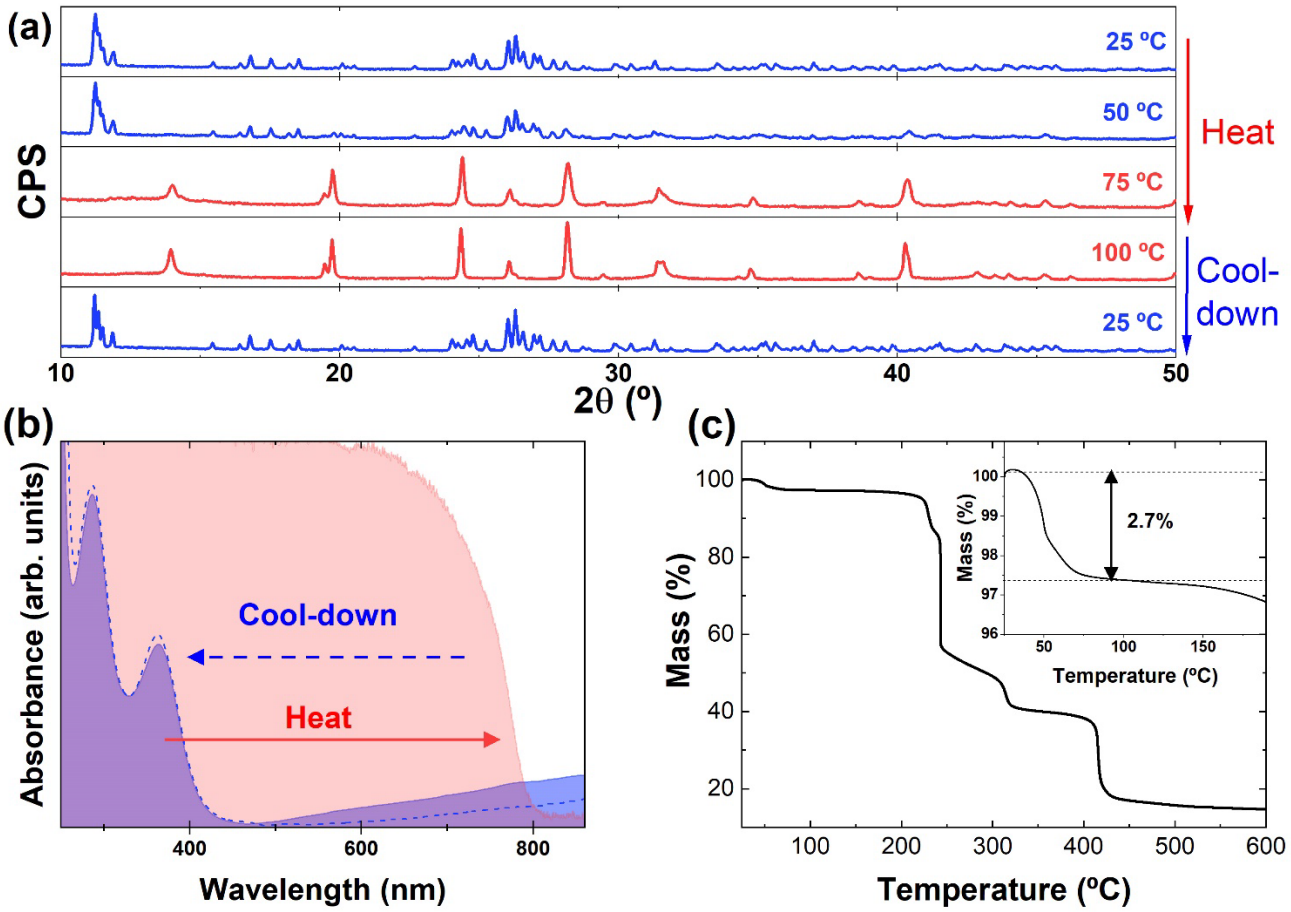

Figure 2. (a) Temperature-dependent X-ray diffractograms of methylammonium lead iodide sample. (b) Optical absorption of pristine methylammonium lead iodide sample (plain blue), as well as after thermal annealing at 100 ºC (red) and upon cool-down to ambient temperature (blue dashes). (c) Thermogravimetric analysis in the 25ºC-600ºC temperature range, with inset focusing on the 25ºC-175ºC range.

The top diffractogram in Figure 3a, recorded at room temperature, corresponds to the 0D phase as detailed above (see Figure 2a and Table 1). When the sample is heated up to 50 ºC, no significant differences are observed, meaning that this phase is stable up to this temperature. However, when thermal annealing is further conducted at 75 ºC and 100 ºC a drastic change occurs, with the vanishing of the characteristic 0D peaks and the rise of new diffraction peaks, especially at 2θ=14.0º, 19.7º, 24.4º, 28.2º, and 40.4º. These can all be ascribed to the cubic phase of $MAPbI_3$[25] with corresponding planes: (001), (011), (111), (002), and (022). We also note the presence of other minor peaks, as for example around 2θ=19.4º in partial overlap with the (011) peak of $MAPbI_3$. This does not seem to belong to either the 3D phase (neither cubic nor tetragonal $MAPbI_3$) nor the 0D one. The most likely explanation

is that it belongs to crystalline CH_3NH_3I (MAI). Indeed, as the 0D and 3D phases are not stoichiometric, the transformation from the former to the latter necessarily involves byproducts. Furthermore, the fate of the water molecules remains unknown. It is possible that they are evaporated (note that evaporation occurs typically below the boiling point). Hence, the easiest and most straightforward reaction mechanism is the following decomposition:

(1) $MA_4PbI_6{\cdot}2H_2O \rightarrow MAPbI_3 + 3\ MAI + 2H_2O(g)$.

Nevertheless, due to the lack of a reliable crystallographic information file for MAI, we cannot guarantee that this simple reaction is the (only) one at play in the transformation observed here.

In any case, the 0D → 3D transformation is also clear from UV-visible absorption spectra (Figure 3b). Indeed, as the powders are heated up to 100 ºC a clear absorption onset forms around 800 nm (*i.e.,* 1.55 eV) as expected for $MAPbI_3$. Moreover, if the powders are left to cool-down at room temperature in ambient air (relative humidity around 40-60%) for one week, both the XRD (Figure 3a, bottom diffractogram) and absorption properties of the material return to the original ones for the as-synthesized 0D phase.

To gain more detailed insights into the mechanisms involved in these transformations we performed thermogravimetric analysis (TGA; Figure 3c) of as-synthesized $MA_4PbI_6{\cdot}2H_2O$. If we focus on the 25ºC-150ºC temperature range (higlighted as inset in Figure 3c) we observe a mass loss of about 2.7% around 50ºC-75ºC. This loss, which corresponds to the 0D→3D transformation observed by XRD is consistent with the loss of 2 water molecules (36 g/mol) out of each $MA_4PbI_6{\cdot}2H_2O$ unit (1121 g/mol). Again, this points out to the complete loss of water by evaporation at these relatively low temperatures (and not the formation of liquid water or other hydrated or solvated compounds). It is also clear that the dehydration causes the collapse of the 0D structure which is unstable without the corresponding water molecules (as also observed when direct synthesis is attempted in dry nitrogen; Figure S1). The fact that no further weight loss is observed up to 100 ºC explains that a reversed hydration in ambient

air may be sufficient to recover the 0D phase, as previously observed. A further look at the TGA signal suggests that the reversibility may be preserved up to around 200 ºC. However, beyond that temperature, many mass losses are observed. Indeed, the decomposition mechanism of methylammonium lead iodide can be quite complex and give rise to different species such as CH_3NH_2 and HI or other.[26,27]

Eventually, given the high phase purity observed on the direct mechanochemical synthesis of MA_4PbI_6 and the promising conversion into the 3D perovskite counterpart described so far, we decided to expand the material compositions to $MA_4PbBr_6 \cdot 2H_2O$ and mixed-halide $MA_4Pb(I:Br)_6 \cdot 2H_2O$ with

different I:Br ratios. Indeed, mixed-halide compositions have been demonstrated to be very interesting in ternary metal halides to tune the structural and/or optoelectronic properties.

Figure 4a presents the XRD patterns of a series of $MA_4Pb(I_xBr_{1-x})_6 \cdot 2H_2O$ compounds and corresponding fits.

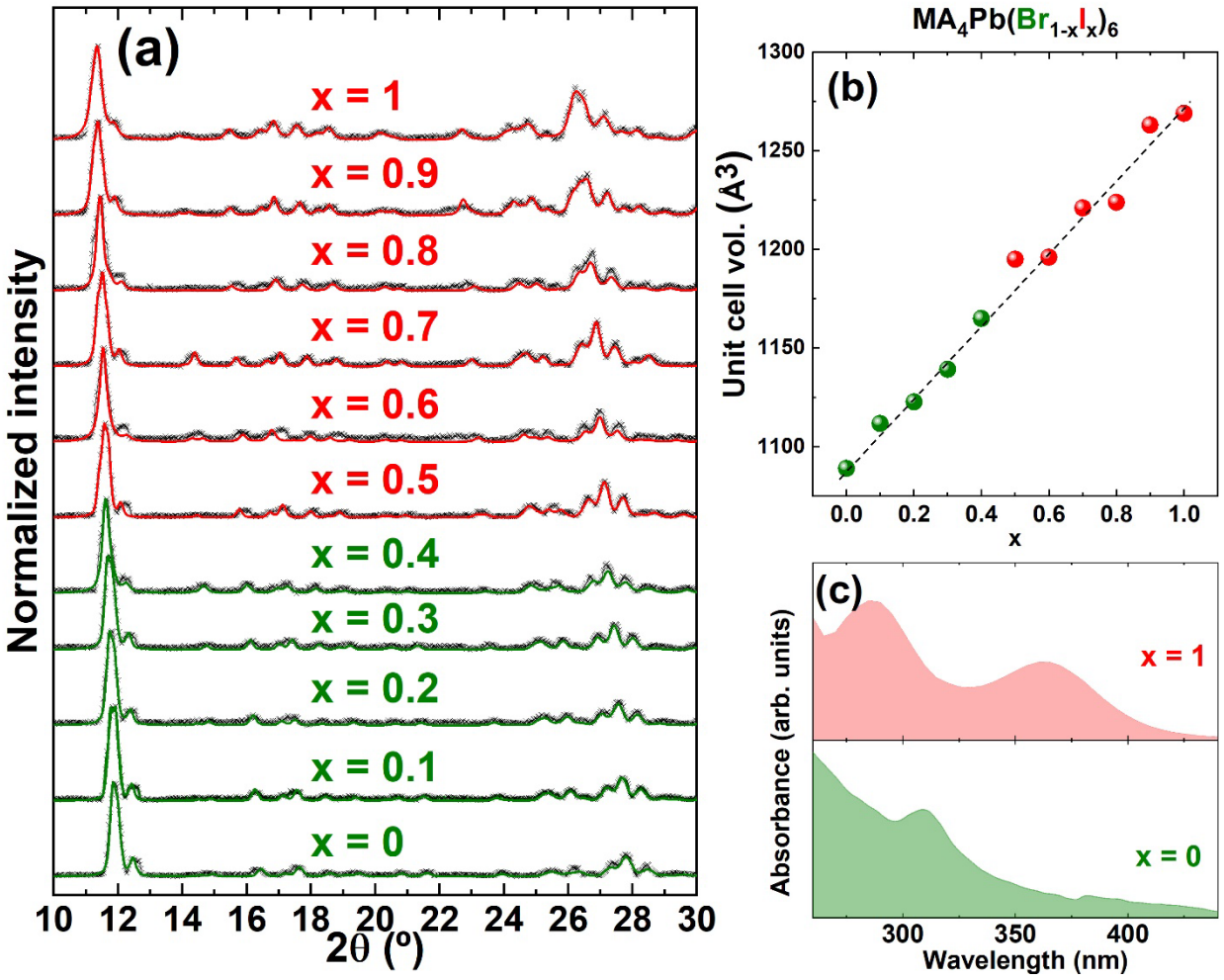

Figure 3. (a) XRD data of $MA_4Pb(Br_{1-x}I_x)_6$ with 0<x<1. (b) Unit cell volume of the I-Br mixture perovskites. (c) UV-visible absorption spectra of pure MA_4PbI_6 and MA_4PbBr_6.

A gradual shift towards higher diffraction angles is observed with decreasing the value of x (see Figure S2 for easier visualization of the main diffraction peak shift). This is expected as the smaller anion Br^- replaces I^- in the structure, hence leading to a contraction of the unit cell. Unit cell volumes derived from Le Bail fits are represented in Figure 4b showing a linear relationship on x. Hence, we conclude that mixed $MA_4Pb(I_xBr_{1-x})_6 \cdot 2H_2O$ zero-dimensional methylammonium lead halides follow a classical Vegaard's law without phase transitions or miscibility gaps. This is in contrast with Cl-based compounds. In fact, we could not form Cl-analogues with this approach (see Figure S3). It may be inferred that Cl^- is too small to stabilize this structure. However, inorganic Cs_4PbX_6 compounds have

been demonstrated with Cl, Br, and I.[19] Hence, the instability of the chloride compounds may reside in the different interactions with water, as we recall that the hybrid organic-inorganic structures are hydrated. The replacement of I for Br in the crystalline structure results in a shift of the lower energy absorption peak (Figure 4c) from 364nm to 310nm, similar to what is observed on the inorganic analogues.[19] For mixed iodide-bromide compounds, it could be expected that the absorption spectra showed features of both compositions resulting in a broader signal. This is because in such zero-dimensional structures absorption comes from localized states in single octahedra, as explained elsewhere.[19] In our case we found that the absorption spectrum of the mixed I-Br compound was dominated by the absorption of PbI_6 octahedra with no visible contribution from the bromide part (see Figure S4). We hypothesize that this may be due to a significantly higher absorption coefficient from $MA_4PbI_6{\cdot}2H_2O$ compared to $MA_4PbBr_6{\cdot}2H_2O$. Nevertheless, it is worth noting that the 0D to 3D conversion upon annealing also occurs for bromide and mixed iodide-bromide compositions and this results in tunable bandgaps in the visible range (see Figure S5).

METHODS:

Materials. Methylammonium iodide (MAI, > 99.5 %), methylammonium bromide (MABr, > 99.5 %), and lead(II) iodide (PbI_2, ≥ 99.999 %) were purchased from Lumtec. Lead(II) bromide ($PbBr_2$, ≥ 98 %) were purchased from TCI. All chemicals were stored in a nitrogen-filled glovebox and used as received without further purification.

Mechanochemical synthesis of $MA_4Pb(Br_{1-x}I_x)_6{\cdot}2H_2O$ powders. MAI:MABr:PbI_2:$PbBr_2$ powders (X = Cl, Br, or I) were weighted inside a nitrogen-filled glovebox. Then, approximately 2 grams of the mixed precursors powders was introduced and closed inside 10 mL zirconia ball-mill jars with 2 zirconia beads of 10 mm in diameter under ambient atmosphere to introduce moisture. Then ball-milling was performed with a MM-400 straight ball-mill from Retsch, at a frequency of 30 Hz for 1 hour.

XRD characterization. X-ray diffraction was measured with a Panalytical Empyrean diffractometer equipped with CuKα anode operated at 45 kV and 40 mA and a Pixel 1D detector in scanning line mode. Single scans were acquired in the 2 theta = 10° to 50° range in Bragg-Brentano geometry in air. The annealing of the powder was performed in-situ with a custom-made heating platform. Heating was performed at approximately 7ºC/min and the temperature was left constant for 5 min at each step before starting the data acquisition. Data analysis, and in particular Le Bail whole-pattern fits, was performed with Fullprof software.

Optical characterization. For optical absorbance measurements, powders were dispersed in an ethanol:hexane (1:3) solution. Absorbance spectra were then collected with a Perkin-Elmer UV/Visible spectrometer, applying a background correction (blank) for the neat solvent mixture.

Thermogravimetric analysis (TGA). The TGA measurements were performed with a TGA550 from TA instruments and a temperature step size of 20.0°C/min.

CONCLUSION:

In summary, zero-dimensional $MA_4Pb(Br_{1-x}I_x)_6 \cdot 2H_2O$ powders ($0<x<1$) with sharp and tunable absorption features in the near UV have been successfully synthesized by a simple mechanochemical approach. Structural characterization reveals the high-purity and good halide-mixing of all compounds. Furthermore, thermal annealing in air at moderate temperatures (around 75ºC) triggers a drastic transformation from the zero-dimensional phase into the 3D perovskite analogue, with strong absorption throughout the whole visible range. This transformation is reversible by simply cooling-down of the sample in air. These results, especially on the reversible phase transformations are rationalized by a (de)hydration mechanism. Indeed, contrary to what is reported for the inorganic Cs_4PbX_6 counterparts, water is an essential part of the –dihydrate– hybrid organic-inorganic $MA_4PbX_6 \cdot 2H_2O$ compounds; in other words, non-hydrated MA_4PbX_6 does not appear to be thermodynamically stable. Our results pave the way to a better understanding of the phase transformations of ternary metal halides which have so far only been extensively studied for Cs-based inorganic compounds.

ASSOCIATED CONTENT

Supporting Information

X-ray diffractograms and UV-Visible absorption spectra.

ACKNOWLEDGEMENTS

We thank Ignacio Rosa Pardo and Raquel Galian for assistance with the optical characterization measurements. The research leading to these results has received funding from the European Research Council (ERC) under the European Union's Horizon 2020 research and innovation programme (Grant agreement No. 834431) and the Spanish Ministry of Science, Innovation and Universities (MICIU, MAT2017-88821-R, PCI2019-111829-2 and EQC2018-004888-P) and the

Comunitat Valenciana (IDIFEDER/2018/061 and Prometeu/2020/077). F. P. also acknowledges the Spanish Ministry of Science for his Juan de la Cierva contract.

REFERENCES

(1) Toso, S.; Baranov, D.; Manna, L. Hidden in Plain Sight: The Overlooked Influence of the Cs + Substructure on Transformations in Cesium Lead Halide Nanocrystals . *ACS Energy Lett.* **2020**, 3409–3414.

(2) Stranks, S. D.; Snaith, H. J. Metal-Halide Perovskites for Photovoltaic and Light-Emitting Devices. *Nat. Nanotechnol.* **2015**, *10* (5), 391–402.

(3) Park, N. G. Perovskite Solar Cells: An Emerging Photovoltaic Technology. *Mater. Today* **2015**, *18* (2), 65–72.

(4) Assadi, M. K.; Bakhoda, S.; Saidur, R.; Hanaei, H. Recent Progress in Perovskite Solar Cells. *Renew. Sustain. Energy Rev.* **2018**, *81* (May 2017), 2812–2822.

(5) Quarti, C.; Katan, C.; Even, J. Physical Properties of Bulk, Defective, 2D and 0D Metal Halide Perovskite Semiconductors from a Symmetry Perspective. *J. Phys. Mater.* **2020**, *3* (4), 042001.

(6) Saidaminov, M. I.; Almutlaq, J.; Sarmah, S.; Dursun, I.; Zhumekenov, A. A.; Begum, R.; Pan, J.; Cho, N.; Mohammed, O. F.; Bakr, O. M. Pure Cs4PbBr6: Highly Luminescent Zero-Dimensional Perovskite Solids. *ACS Energy Lett.* **2016**, *1* (4), 840–845.

(7) Saidaminov, M. I.; Mohammed, O. F.; Bakr, O. M. Low-Dimensional-Networked Metal Halide Perovskites: The next Big Thing. *ACS Energy Lett.* **2017**, *2* (4), 889–896.

(8) Akkerman, Q. A.; Park, S.; Radicchi, E.; Nunzi, F.; Mosconi, E.; De Angelis, F.; Brescia, R.; Rastogi, P.; Prato, M.; Manna, L. Nearly Monodisperse Insulator Cs4PbX6 (X = Cl, Br, I) Nanocrystals, Their Mixed Halide Compositions, and Their Transformation into CsPbX3 Nanocrystals. *Nano Lett.* **2017**, *17* (3), 1924–1930.

(9) Akkerman, Q. A.; Abdelhady, A. L.; Manna, L. Zero-Dimensional Cesium Lead Halides: History, Properties and Challenges. **2018**.

(10) Riesen, N.; Lockrey, M.; Badek, K.; Riesen, H. On the Origins of the Green Luminescence in

the “Zero-Dimensional Perovskite” Cs4PbBr6: Conclusive Results from Cathodoluminescence Imaging. *Nanoscale* **2019**, *11* (9), 4001–4007.

(11) Wang, L.; Liu, H.; Zhang, Y.; Mohammed, O. F. Photoluminescence Origin of Zero-Dimensional Cs4PbBr6 Perovskite. *ACS Energy Lett.* **2020**, *5* (1), 87–99.

(12) Nguyen, L. A. T.; Minh, D. N.; Yuan, Y.; Samanta, S.; Wang, L.; Zhang, D.; Hirao, N.; Kim, J.; Kang, Y. Pressure-Induced Fluorescence Enhancement of FAαPbBr2+α Composite Perovskites. *Nanoscale* **2019**, *11* (13), 5868–5873.

(13) Sharma, S. K.; Phadnis, C.; Das, T. K.; Kumar, A.; Kavaipatti, B.; Chowdhury, A.; Yella, A. Reversible Dimensionality Tuning of Hybrid Perovskites with Humidity: Visualization and Application to Stable Solar Cells. *Chem. Mater.* **2019**, *31* (9), 3111–3117.

(14) Vincent, B. R.; Robertson, K. N.; Cameron, T. S.; Knop, O. Alkylammonium Lead Halides. Part 1. Isolated PbI64- Ions in (CH3NH3)4PbI6·2H2O. *Can. J. Chem.* **1987**, *65* (5), 1042–1046.

(15) Leguy, A. M. A.; Hu, Y.; Campoy-Quiles, M.; Alonso, M. I.; Weber, O. J.; Azarhoosh, P.; Van Schilfgaarde, M.; Weller, M. T.; Bein, T.; Nelson, J.; Docampo, P.; Barnes P. R. F. Reversible Hydration of CH3NH3PbI3 in Films, Single Crystals, and Solar Cells. *Chem. Mater.* **2015**, *27* (9), 3397–3407.

(16) Song, Z.; Watthage, S. C.; Phillips, A. B.; Tompkins, B. L.; Ellingson, R. J.; Heben, M. J. Impact of Processing Temperature and Composition on the Formation of Methylammonium Lead Iodide Perovskites. *Chem. Mater.* **2015**, *27* (13), 4612–4619.

(17) Li, J.; Zhang, H.; Wang, S.; Long, D.; Li, M.; Wang, D.; Zhang, T. Inter-Conversion between Different Compounds of Ternary Cs-Pb-Br System. *Materials (Basel).* **2018**, *11* (5), 1–9.

(18) Palazon, F.; Almeida, G.; Akkerman, Q. A.; De Trizio, L.; Dang, Z.; Prato, M.; Manna, L. Changing the Dimensionality of Cesium Lead Bromide Nanocrystals by Reversible Postsynthesis Transformations with Amines. *Chem. Mater.* **2017**, *29* (10), 4167–4171.

(19) Akkerman, Q. A.; Park, S.; Radicchi, E.; Nunzi, F.; Mosconi, E.; De Angelis, F.; Brescia, R.; Rastogi, P.; Prato, M.; Manna, L. Nearly Monodisperse Insulator Cs4PbX6(X = Cl, Br, I) Nanocrystals, Their Mixed Halide Compositions, and Their Transformation into CsPbX3Nanocrystals. *Nano Lett.* **2017**, *17* (3), 1924–1930.

(20) Udayabhaskararao, T.; Houben, L.; Cohen, H.; Menahem, M.; Pinkas, I.; Avram, L.; Wolf, T.;

Teitelboim, A.; Leskes, M.; Yaffe, O.; Oron, D; Kazes, M. A Mechanistic Study of Phase Transformation in Perovskite Nanocrystals Driven by Ligand Passivation. *Chem. Mater.* **2018**, *30* (1), 84–93.

(21) Liu, Z.; Bekenstein, Y.; Ye, X.; Nguyen, S. C.; Swabeck, J.; Zhang, D.; Lee, S. T.; Yang, P.; Ma, W.; Alivisatos, A. P. Ligand Mediated Transformation of Cesium Lead Bromide Perovskite Nanocrystals to Lead Depleted Cs4PbBr6 Nanocrystals. *J. Am. Chem. Soc.* **2017**, *139* (15), 5309–5312.

(22) Palazon, F.; Ajjouri, Y. El; Bolink, H. J. Making by Grinding : Mechanochemistry Boosts the Development of Halide Perovskites and Other Multinary Metal Halides. *Adv. Energy Mater.* **2019**, *1902499*, 1–13.

(23) Karmakar, A.; Dodd, M. S.; Zhang, X.; Oakley, M. S.; Klobukowski, M.; Michaelis, V. K. Mechanochemical Synthesis of 0D and 3D Cesium Lead Mixed Halide Perovskites. *Chem. Commun.* **2019**, *55* (35), 5079–5082.

(24) De Bastiani, M.; Dursun, I.; Zhang, Y.; Alshankiti, B. A.; Miao, X. H.; Yin, J.; Yengel, E.; Alarousu, E.; Turedi, B.; Almutlaq, J. M.; Saidaminov, M. I.; Mitra, S.; Gereige, I.; Alsaggaf, A.; Zhu Y.; Han, Y.; Roqan, I. S.; Bredas, J.-L.; Mohammed, O. F.; Bakr, O. M. Inside Perovskites: Quantum Luminescence from Bulk Cs4PbBr6Single Crystals. *Chem. Mater.* **2017**, *29* (17), 7108–7113.

(25) Jacobsson, T. J.; Schwan, L. J.; Ottosson, M.; Hagfeldt, A.; Edvinsson, T. Determination of Thermal Expansion Coefficients and Locating the Temperature-Induced Phase Transition in Methylammonium Lead Perovskites Using X-Ray Diffraction. *Inorg. Chem.* **2015**, *54* (22), 10678–10685.

(26) Juarez-Perez, E. J.; Hawash, Z.; Raga, S. R.; Ono, L. K.; Qi, Y. Thermal Degradation of CH3NH3PbI3 Perovskite into NH3 and CH3I Gases Observed by Coupled Thermogravimetry-Mass Spectrometry Analysis. *Energy Environ. Sci.* **2016**, *9* (11), 3406–3410.

(27) Abdelmageed, G.; Mackeen, C.; Hellier, K.; Jewell, L.; Seymour, L.; Tingwald, M.; Bridges, F.; Zhang, J. Z.; Carter, S. Effect of Temperature on Light Induced Degradation in Methylammonium Lead Iodide Perovskite Thin Films and Solar Cells. *Sol. Energy Mater. Sol. Cells* **2018**, *174* (February 2017), 566–571.

TOC graphic

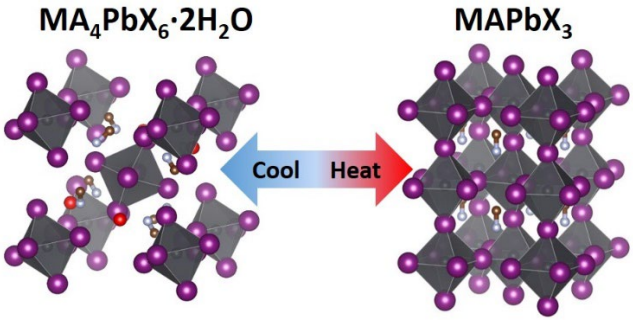

Zero-dimensional hydrated methylammonium lead halides with narrow-band absorption in the UV are mechanochemically synthesized with different anion compositions. It is furthermore demonstrated that these structures undergo a reversible phase transformation into three-dimensional perovskites with broadband absorption throughout the visible range. These transformations occur upon simple heating in air and are shown to be linked to the desorption of water and consequent collapse of the zero-dimensional structure, contrary to what is observed on inorganic counterparts (Cs_4PbX_6).

Supporting Information for:

Zero-dimensional hybrid organic-inorganic lead halides and their post-synthesis reversible transformation into 3D perovskites

Bas A. H. Huisman, Francisco Palazon,* and Henk J. Bolink

Instituto de Ciencia Molecular, Universidad de Valencia, C/ Catedrático J. Beltrán 2, 46980, Paterna, Spain. E-mail: francisco.palazon@uv.es

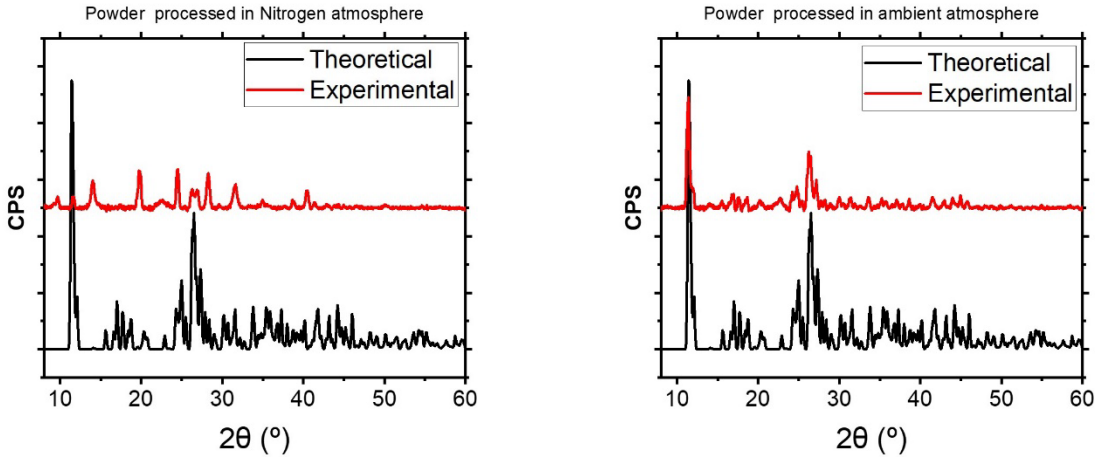

Figure S 1. X-ray diffraction patterns of ball-milled MAI:PbI_2 in 4:1 ratio in nitrogen (left panel, red) and air (right panel, red), compared to the theoretical pattern of MA4PbI6·$2H_2O$ (black). Only when ball-milling is performed in air the experimental pattern shows a good match with the expected 0D phase.

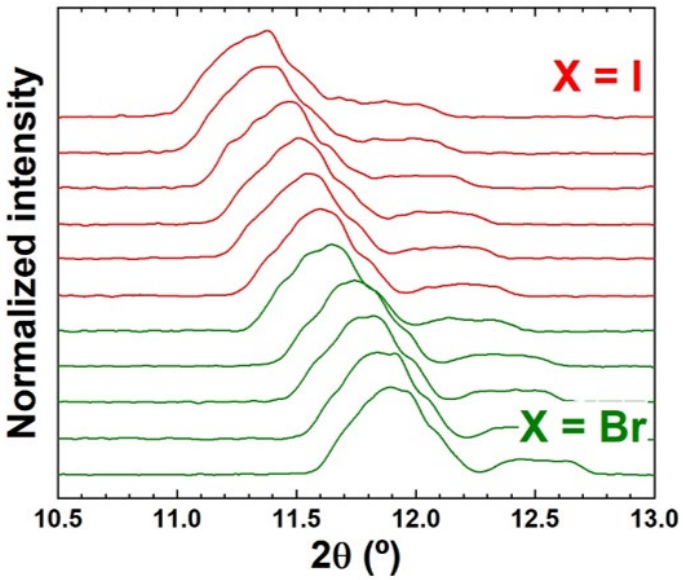

Figure S 2. X-ray diffractograms of $MA_4Pb(Br_{1-x}I_x)_6 \cdot 2H_2O$. Top diffractogram corresponds to x=1 and bottom one to x=0. This is a closer view on the low-angle part of the data presented in the main text (Figure 4b) for a better visualization of the diffraction signal shift corresponding to the unit cell expansion with the gradual replacement of bromide with iodide anions.

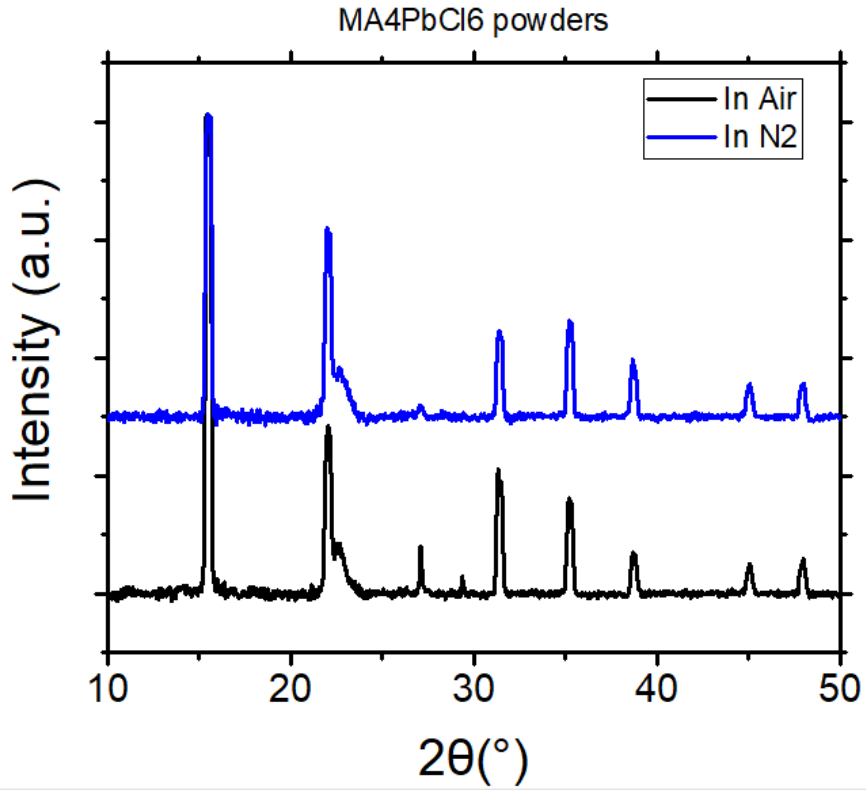

Figure S 3. X-ray diffraction pattern of ball-milled MACl:$PbCl_2$ powders in 4:1 molar ratio in air and nitrogen. In both cases the observed phase corresponds to $MAPbCl_3$.

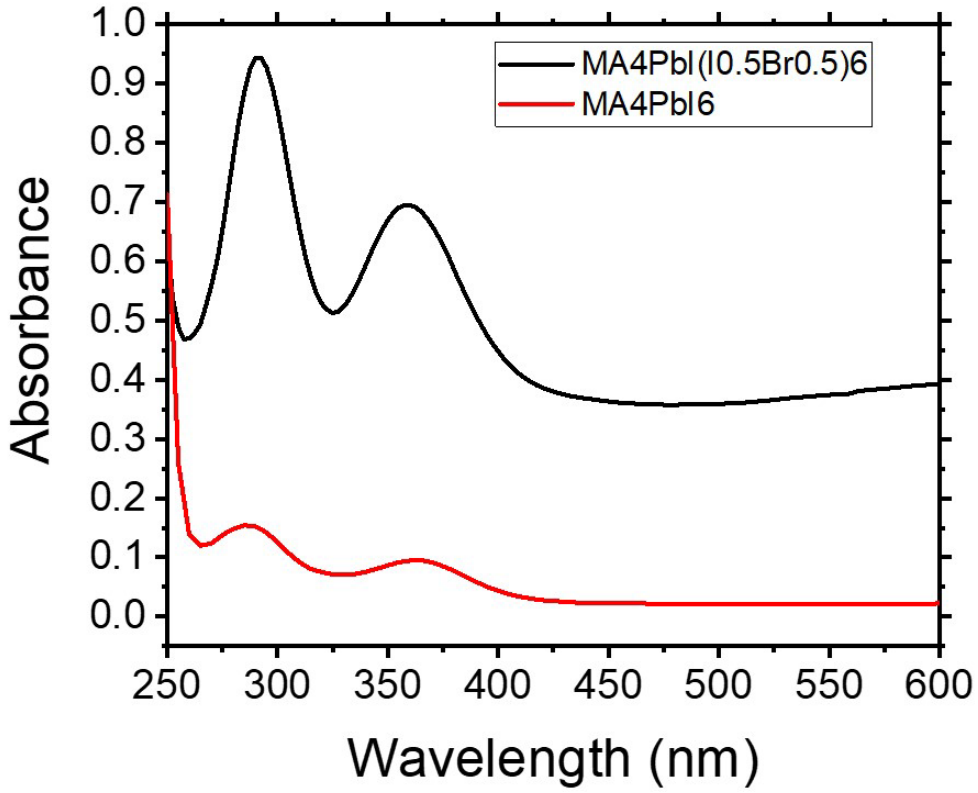

Figure S 4. UV absorption spectra of $MA_4Pb(Br_{0.5}I_{0.5})_6 \cdot 2H_2O$ and $MA_4PbI_6 \cdot 2H_2O$ showing nearly identical features. This is not the case for 3D compounds after annealing (see Figure S5).

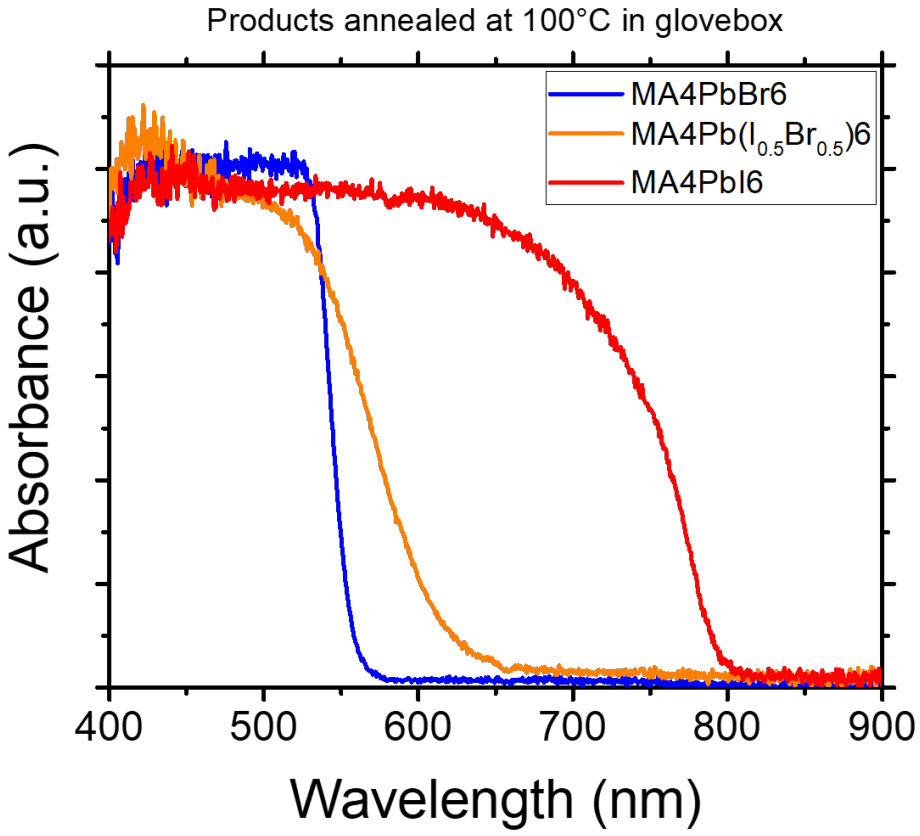

Figure S 5. Absorption spectra of annealed powders with different compositions, showing the formation of three-dimensional perovskties MAPbBr3 (blue), MAPbI3 (red), and mixed MAPb(I:Br)3 (orange).